Gene Delivery in Three-Dimensional Cell Cultures by Superparamagnetic Nanoparticles

Haiyuan Zhang,[†] Moo-Yeal Lee,[‡] Michael G. Hogg,[‡] Jonathan S. Dordick,[†] and Susan T. Sharfstein[†,§,*]

[†]Department of Chemical and Biological Engineering and Center for Biotechnology and Interdisciplinary Science, Rensselaer Polytechnic Institute, Troy, New York 12180 and [‡]Solidus Biosciences, Inc., San Francisco, California 94158. [§]Current address: College of Nanoscale Science and Engineering, University at Albany, Albany, NY 12203.

ABSTRACT Three-dimensional (3D) cellular assays closely mimic the *in vivo* milieu, providing a rapid, inexpensive system for screening drug candidates for toxicity or efficacy in the early stages of drug discovery. However, 3D culture systems may suffer from mass transfer limitations, particularly in delivery of large polypeptide or nucleic acid compounds. Nucleic acids (*e.g.*, genes, silencing RNA) are of particular interest both as potential therapeutics and due to a desire to modulate the gene-expression patterns of cells exposed to small-molecule pharmacological agents. In the present study, polyethylenimine (PEI)-coated superparamagnetic nanoparticles (SPMNs) were designed to deliver interfering RNA and green fluorescent protein (GFP) plasmids through a collagen−gel matrix into 3D cell cultures driven by an external magnetic field. The highest transfection efficiency achieved was 64% for siRNA and 77% for GFP plasmids. Delivery of an shRNA plasmid against GFP by PEI-coated SPMNs silenced the GFP expression with 82% efficiency. We further demonstrated that this delivery approach could be used for screening interfering RNA constructs for therapeutic or toxic effects for cells grown in 3D cultures. Four known toxic shRNA plasmids were delivered by PEI-coated SPMNs into 3D cell cultures, and significant toxicities (41−51% cell death) were obtained.

KEYWORDS: gene expression · gene transfer · cytotoxicity · magnetism · silencing RNA

Advances in genomics and proteomics have provided a wide range of new pharmacological targets for the drug discovery process.[1−5] However, these new targets have not yielded a wealth of new pharmaceuticals. In fact, the drug discovery process is an investment-intensive, high-risk endeavor that results in low yields of effective and safe drugs. In 2005, investment in pharmaceutical research and development was approximately $40 billion, which led to 20 new drugs approved by the FDA. Similarly, in the biopharmaceutical industry, approximately $20 billion was spent on research and development in 2005, with seven new drugs approved by the FDA.[6−9] One problem in early stage drug discovery is that traditional two-dimensional (2D) monolayer cellular assays often used cannot accurately predict the preclinical and clinical responses in later stage drug development.[10,11] The low predictability of 2D cellular assays has been partially attributed to poor similarity between the responses of cells present in the *in vivo* milieu and the responses of cells cultured on tissue-culture plastic,[10,11] due to phenotypic differences between cultured cells and those in their native environment that in turn, affect the cellular responses to drugs.[12−14]

To more closely mimic the *in vivo* cell milieu and improve the success rate of drug candidate screening, three-dimensional (3D) cell-based assays have been developed for early stages of the drug discovery process with a goal of more accurately predicting the late-stage clinical responses. These 3D assays will serve to bridge the considerable gap between traditional 2D cellular assays, animal studies, and clinical trials.[15] Recently, a 3D cellular microarray was successfully applied for the screening of small organic molecules, thus demonstrating the ability of 3D human cell cultures to predict accurately the toxicity of both parental compounds and their metabolites.[16]

RNA interference (RNAi) therapeutics are a potential new class of pharmaceutical drugs against a wide range of human diseases, such as cancer, infection, and respiratory disease.[17,18] By silencing the expression of pathological proteins, RNAi is applicable to all classes of molecular targets, including "non-druggable" targets that are difficult to modulate with traditional small-molecule pharmaceutical approaches.[17] Although RNAi screening has been successfully applied in 2D cellular assay platforms,[19−21] it is difficult to apply in 3D cellular assay platforms because RNAi molecules (small interfering (si) RNA or short hairpin (sh)RNA) cannot penetrate the tight gel matrix and enter the 3D cell cultures even with the help of transfection

*Address correspondence to ssharfstein@uamail.albany.edu.

Received for review December 22, 2009 and accepted July 02, 2010.

Published online July 13, 2010.
10.1021/nn9018812

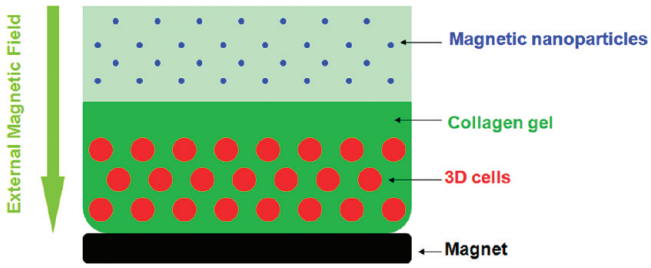

Scheme 1. Delivery of magnetic nanoscale transfection complexes into collagen-based 3D cell cultures

reagents. After evaluating a number of commercially available transfection reagents and determining that they were inefficient at delivering siRNA molecules or shRNA plasmids into 3D cell cultures, we designed and synthesized low-molecular-weight, branched polyethylenimine (PEI)-coated superparamagnetic iron oxide nanoparticles (SPMNs). We then employed these SPMNs to condense siRNA molecules or shRNA plasmids, forming magnetic nanoparticles that were then driven by an external magnetic field to enter a collagen gel matrix (Scheme 1) and transfect cells in a 3D-culture environment, suppressing the expression of target genes.

RESULTS AND DISCUSSION

To facilitate RNAi screening in 3D cell cultures, an efficient carrier is required to deliver nucleic acids through the cell-culture matrix into the cells. We explored a number of commercially available transfection reagents with varying chemistries in an attempt to deliver siRNA or plasmid DNA into cell cultures immobilized in collagen matrices (Table 1). Reagents explored include FuGene HD (Roche), Lipofectamine 2000 (Invitrogen), Effectine (Qiagen), jetPEI (Polyplus transfection), and Deliver X Plus (Panomics), which are composed of cationic lipids, nonliposomal lipids, polymers, or amphipathic peptides, in an attempt to deliver carboxyfluorescein (FAM)-siRNA or green fluorescent protein (GFP) plasmids into 3D cell cultures. However, their transfection efficiencies were very poor. As shown in Figure 1, less than 1% of the cells in the 3D culture were transfected by FuGene HD complexed with FAM-siRNA (Figure 1A) or FuGene HD complexed with GFP plasmid DNA (Figure 1B), despite successful transfection of standard 2D cell cultures with these reagents (data not shown). We hypothesized that the reason for transfection failure was that transfection reagent/nucleic acid complexes were unable to permeate the collagen matrix and access the cells. We then evaluated commercially available transfection reagents based on magnetic nanoparticles (PolyMag, OZ Biosciences, Parc Scientifique Luminy, France), hypothesizing that the external magnetic field could be employed to drive the nucleic acid/magnetic particle complexes into the collagen matrix. While the magnetic nanoparticles showed increased transfection efficiency (Figures 1C,D), the transfection efficiencies for both FAM-siRNA and GFP plasmid were still below 5% (Table 1). Given the large magnetic core size of PolyMag (250 nm), we attributed the low transfection efficiency to the PolyMag/nucleic acid complexes being inhibited by the tight collagen matrix, even under the external magnetic field. We then hypothesized that magnetic nanoparticles with smaller particle size would be more efficient at transfecting cells in 3D cell cultures. Herein, low-molecule-weight, branched polyethylenimine (PEI)-coated superparamagnetic iron oxide nanoparticles (SPMNs) were prepared to condense siRNA or plasmid DNA, forming small particle-size magnetic complexes, and these complexes were employed to transfect cells in 3D cell cultures.

TABLE 1. Transfection Efficiencies of Commercially Available Transfection Reagents in 2D and 3D Cell Cultures

		transfection efficiency (%)	
reagent	manufacturer	2D monolayer culture	3D collagen system
FuGene HD	Roche	90−95	0
Lipofectamine LTX	Invitrogen	90−95	0
HiPerFect	Qiagen	70−80	0
SilMPORTER	Upstate	65−70	0
Effectene	Qiagen	85−90	0
Dreamfect Gold	OZ Biosciences	70−75	0
Deliver X Plus	Panomics	30−40	0
Arrest In	Open Biosystems	80−85	<1
jetPEI	Polyplus-transfection	80−85	<1
PolyMag	OZ Biosciences	75−80	<5

Production and Characterization of PEI-Coated SPMNs and Formation of SPMN-Nucleic Acid Complexes. PEI-coated SPMNs were prepared from oleic acid-coated SPMNs based on a ligand-exchange reaction.[22] PEI, a hydrophilic and multivalent polymeric ligand with abundant amine groups, has a strong affinity for iron oxide nanoparticles due to amine coordination of iron, and is able to di-

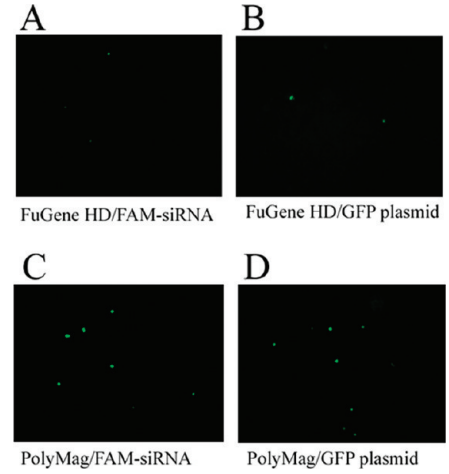

Figure 1. Gene delivery by commercially available FuGene HD and PolyMag into 3D cell cultures. Fluorescent images of 3D cells transfected with (A) FuGene HD/FAM-siRNA; (B) FuGene HD/GFP plasmid; (C) PolyMag/FAM-siRNA, and (D) PolyMag/GFP plasmid. Magnification: 100×.

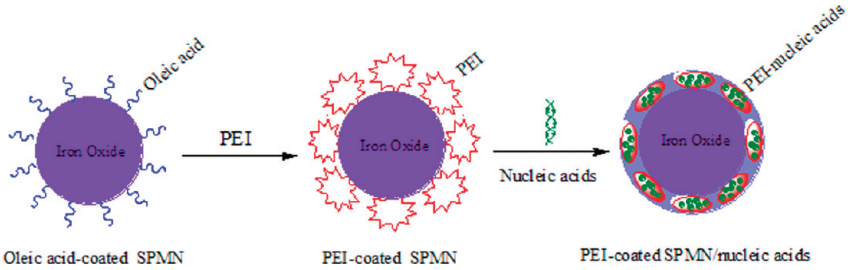

Figure 2. Synthesis of PEI-coated SPMNs.

rectly exchange the hydrophobic oleic-acid ligands from the surface of iron oxide nanoparticles, leading to water-soluble PEI-coated SPMNs (Figure 2). The particle sizes of PEI-coated SPMNs can be controlled by changing the reaction ratios (w/w) of PEI to oleic acid-coated SPMNs (Table 2). Considering the particle size as the potential limiting factor for penetrating the collagen matrix, our objective was to minimize the size of the nanoparticles obtained. Hence, the PEI-coated SPMNs formed at the reaction ratio of 2:1 were adopted in subsequent experiments. The particle size of the PEI-coated SPMNs was determined by transmission electron microscopy (TEM) and dynamic light scattering (DLS), which showed that the core size of the PEI-coated SPMNs was approximately 25−30 nm (Figure 3A) and the corresponding average hydrodynamic size was 36 ± 3 nm (Figure 3B). The zeta potential of the PEI-coated SPMNs was determined to be 46 ± 1.7 mV (Table 2). Compared with the oleic-acid-coated SPMNs that precipitated in water (Figure 3C, left vial), PEI-coated SPMNs had excellent water solubility and could be evenly dispensed in water (Figure 3C, center vial) while still drawn by an external magnetic field (Figure 3C, right vial). The iron and nitrogen contents in PEI-coated SPMNs were determined to be 60.1% and 5.4%, respectively.

PEI-coated SPMNs were used to form transfection complexes with siRNA molecules or GFP plasmids at various N/P (nitrogen from PEI/phosphorus from siRNA or plasmid) ratios. The ability of PEI-coated SPMNs to bind siRNA or plasmid DNA was evaluated by an agarose electrophoresis retardation assay, in which positively charged amino groups in PEI-coated SPMNs will neutralize the negatively charged phosphate groups of siRNA or plasmid DNA, resulting in the loss of electrophoretic mobility of the siRNA or plasmid DNA. Figure 4 shows the result of gel electrophoresis retardation assay in which siRNA at an N/P ratio <27 (Figure 4A) or GFP plasmid at an N/P ratio <18 (Figure 4B) was readily released from transfection complexes. With increasing N/P ratios, the electrophoretic mobility of the siRNA or GFP plasmid was gradually retarded, indicating the increased binding of the PEI-coated SPMNs to siRNA or GFP plasmid DNA. When the N/P ratio of the PEI-coated SPMNs/siRNA reached 27 and that of PEI-coated SPMNs/GFP plasmid reached 18, no free siRNA or GFP plasmid bands were observed on the gel, indicating the siRNA molecules or GFP plasmids were completely complexed by the PEI-coated SPMNs. Generally, PEI has abundant amine groups and can completely bind oligonucleotides or plasmid DNA at N/P ratios of 9−13.[23] Here the higher N/P ratios required by the PEI-coated SPMN-nucleic acid complexes are due to some of the amine groups of PEI being used to coordinate the iron in the superparamagnetic nanoparticles. This observation is reinforced by analysis of the zeta potentials and particle size for the complexed particles (Supporting Information, Table S1) in which the zeta potential changes from negative to positive at an N/P ratio of 27 for siRNA and 18 for GFP plasmid DNA. The minimum particle size occurred at an N/P ratio of 33 for siRNA (41 ± 2 nm) and an N/P ratio of 24 for GFP plasmid DNA (44 ± 2 nm).

TABLE 2. Hydrodynamic Particle Sizes and Zeta Potentials of PEI-Coated SPMNs Formed at Varying Reaction Ratios

reaction ratio (PEI/SPMNs, w/w)	hydrodynamic particle size (nm)	zeta potential (mV)
2:1	36 ± 3	46 ± 1.7
5:1	44 ± 2	54 ± 1.6
10:1	56 ± 3	71 ± 2.1

Transfection Efficiencies for Delivery of siRNA and Plasmid DNA to Cells Cultured in Collagen Matrices. On the basis of the results of the gel electrophoresis retardation assay, transfection complexes of PEI-coated SPMNs/siRNA were prepared at high N/P ratios (27, 30, 33, 36, and 39) to form more stable complexes. Similarly, transfection complexes of PEI-coated SPMNs/GFP plasmid were prepared at high N/P ratios (18, 21, 24, 27, and 30). The transfection complexes with varying N/P ratios were applied to 3D cultures of NIH 3T3 cells immobilized in a collagen gel. An external magnetic field was applied to drive the magnetic complexes through the gel matrix to allow the nucleic acids to enter the cells in the 3D-culture system (Scheme 1). The exposure time of external magnetic field was varied from 1 to 4 h. The transfection efficiency was evaluated by both fluorescence microscopy and flow cytometric analysis.

For siRNA delivery, FAM-labeled siRNA (FAM-siRNA) was used to allow evaluation of the transfection efficiency. With increasing exposure times to the external magnetic field, the transfection efficiencies of the various magnetic transfection complexes gradually increased, reaching a maximum at 3 h; further increases in exposure time (4 h) led to a decrease in transfection

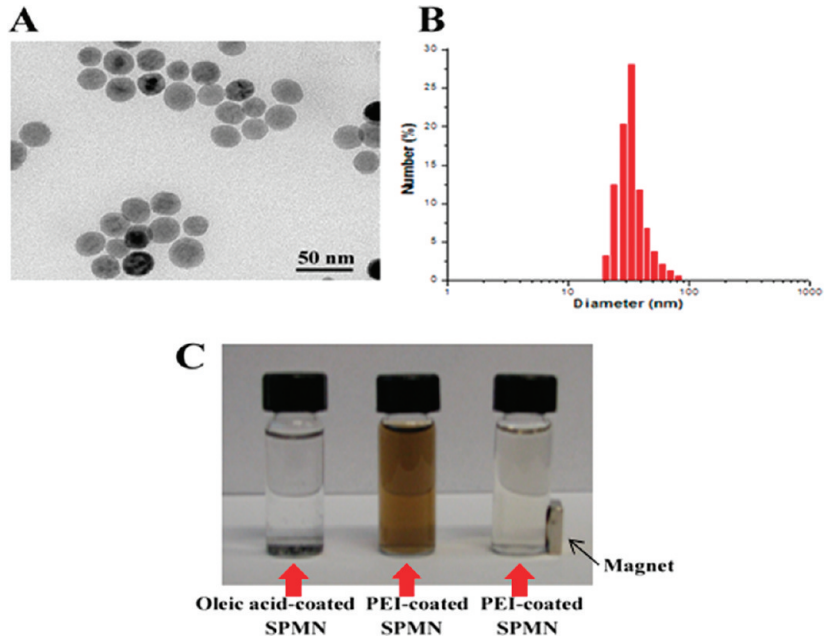

Figure 3. Characterization of PEI-coated SPMN: (A) transmission electron micrograph (TEM) of PEI-coated SPMNs; (B) hydrodynamic size distribution of PEI-coated SPMNs measured by dynamic light scattering (DLS); (C) solubility of oleic acid-coated SPMNs and PEI-coated SPMNs in aqueous solution. The insoluble oleic acid-coated SPMNs precipitate and settle on the bottom (left vial) while the soluble PEI-coated SPMNs yield a brown color (center vial) that can be eliminated by removing the particles from solution with a magnet (right vial).

efficiency (Figure 5A,B) while transfection without exposure to the external magnetic field resulted in virtually no transfection (data not shown). This result indicates the external magnetic field can significantly affect transfection efficiencies of siRNA into 3D cell cultures. Among the stable transfection complexes formed at varying N/P ratios, the complex formed at an N/P ratio of 33 showed the highest transfection efficiency (64 ± 5% by fluorescence microscopy (Figure 5A,C); 62 ± 6% by flow cytometric analysis (Figure 5B,D)). The corresponding hydrodynamic particle size and zeta potential of this complex were 41 ± 2 nm and 37 ± 1.6 mV (Supporting Information, Table S1), respectively. For GFP plasmid delivery, transfection complexes were transfected in a similar manner as for FAM-siRNA, except 24 h of additional incubation was employed after removal of the magnetic plate to allow GFP to be adequately expressed in 3D cell cultures. Fluorescence microscopy images indicated that the transfection efficiencies of the plasmid DNA transfection complexes also gradually increased with increasing exposure time to the magnetic field reaching a maximum at 3 h (Figure 6A,B), similar to the result obtained for siRNA delivery. Further increasing the exposure time (4 h) similarly led to a decrease in transfection efficiency. Among the transfection complexes formed at various N/P ratios, the complex formed at an N/P ratio of 24 showed the highest transfection efficiency (77 ± 6% by fluorescence microscopy (Figure 6A,C); 76 ± 8% by flow cytometric analysis (Figure 6B,D)), and its corresponding hydrodynamic particle size and zeta potential were 44 ± 2 nm and 26 ± 0.8 mV (Supporting Information, Table S1), respectively. Here again, the application of the external magnetic field significantly enhanced the trans-

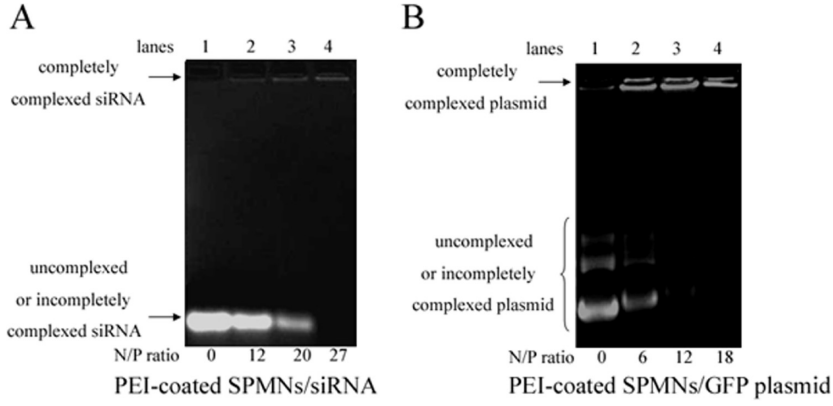

Figure 4. Gel electrophoresis retardation assay. (A) siRNA complexed with PEI-coated SPMNs at an N/P ratio of 0 (lane 1), 12 (lane 2), 20 (lane 3), and 27 (lane 4); (B) GFP plasmid complexed with PEI-coated SPMNs at an N/P ratio of 0 (lane 1), 6 (lane 2), 12 (lane 3), and 18 (lane 4).

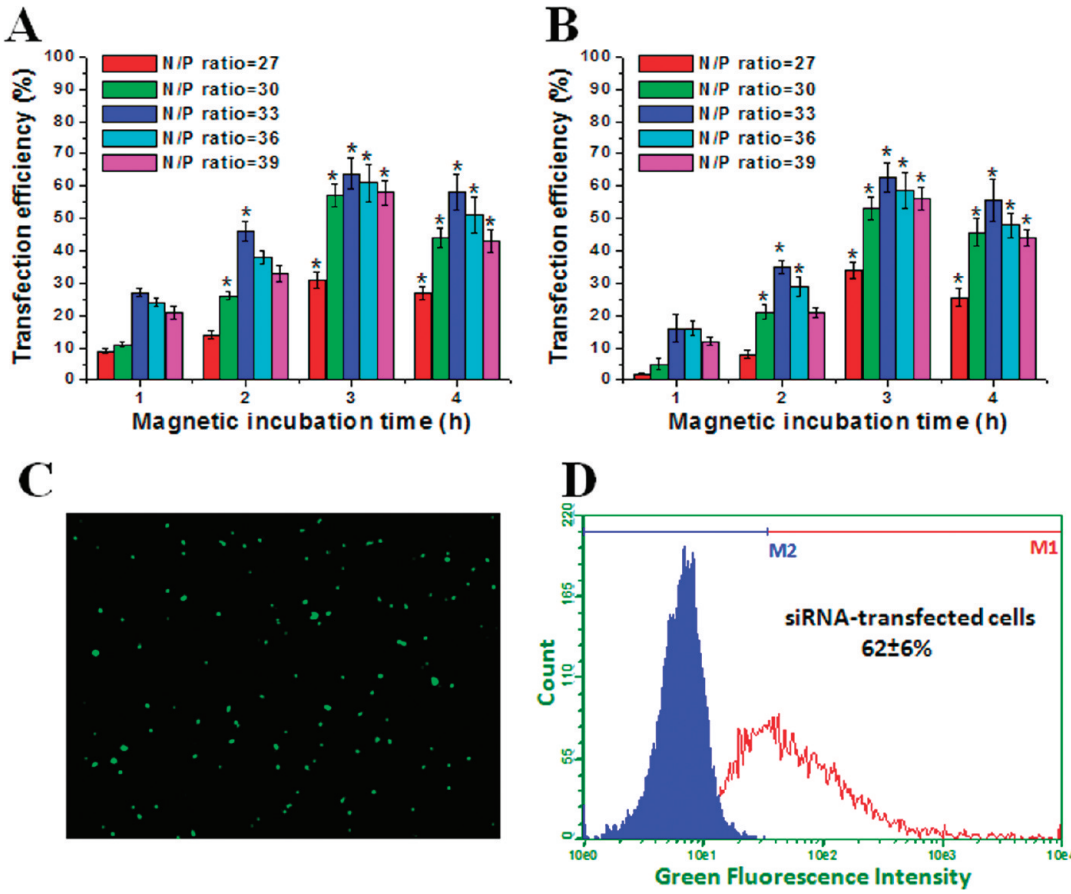

Figure 5. siRNA delivery by PEI-coated SPMNs in 3D cell cultures: (A) transfection efficiency for FAM-siRNA at magnetic incubation time and various N/P ratios determined by fluorescence microscopy; (B) transfection efficiency for FAM-siRNA at magnetic incubation time and various N/P ratios determined by flow cytometric analysis; (C) fluorescent microscopy image of 3D cell cultures transfected by PEI-coated SPMNs/FAM-siRNA at N/P ratio of 33 for 3 h; magnification, 100×; (D) flow cytometric analysis of 3D cell cultures transfected by PEI-coated SPMNs/FAM-siRNA at N/P ratio of 33 for 3 h. Error bars represent the standard deviation of triplicate biological measurements. The asterisks (*) denote a statistical significance at $P <$ 0.005 relative to transfection efficiency at the corresponding N/P ratio at 1 h.

fection efficiencies of the magnetic transfection complexes in 3D cell cultures. As with siRNA, extended exposure time led to a decrease in transfection efficiency, possibly due to some of the magnetic transfection complexes being driven all the way through the collagen matrices so that they could not release the nucleic acids inside the 3D cell cultures. Estimates of transfection efficiency from fluorescence microscopy and flow cytometry were in good agreement for measurements taken after 3 or 4 h of magnetic field exposure. However, for measurements taken after 1 or 2 h of magnetic field exposure, flow cytometric analysis consistently indicated lower transfection efficiencies. We hypothesized that this was due to incomplete penetration of the complexes into the entire 3D culture (~2 mm depth) at the earlier times, whereas at later times, complete penetration permitted homogeneous transfection. Confocal microscopy verified that this was indeed the case (Supporting Information, Figure S2). To determine the maximum penetration depth, confocal microscopy with *Z* sectioning was performed (Figure 7). *Z* stack analysis showed that the maximum transfection depth into the 3D collagen gel cultures was ~2.1−2.3 mm after 3 h of exposure to the external magnetic field; further exposure did not increase the depth of transfection (data not shown). Subsequent cultures were limited to ~1.9 mm in depth to ensure homogeneous transfection in the entire 3D cell culture. The homogeneous transfection to a depth of ~2 mm at 3 h indicates that transfection efficiency of SPMN complexes can be reliably evaluated by fluorescence microscopy image analysis; thus, by combining transfection with SPMNs and fluorescence microscopy, a rapid and efficient tool for screening the transfection efficiency and biological effects of various nucleic acids in 3D cultures can be developed.[16,24]

Application of PEI-Coated SPMNs to Gene Silencing. As we had demonstrated that PEI-coated SPMNs could be used to deliver nucleic acids into 3D cell cultures with high efficiency, we next evaluated whether these complexes could be used for gene silencing by RNAi, a powerful tool that has been extensively applied in 2D cellular assays. A GFP shRNA plasmid that had been previously shown to effectively silence GFP in 2D cell cultures (data not shown) was used to form transfection complexes with PEI-coated SPMNs at various N/P ratios (>18). The resulting magnetic transfection complexes were applied to 3D cell cultures that had been

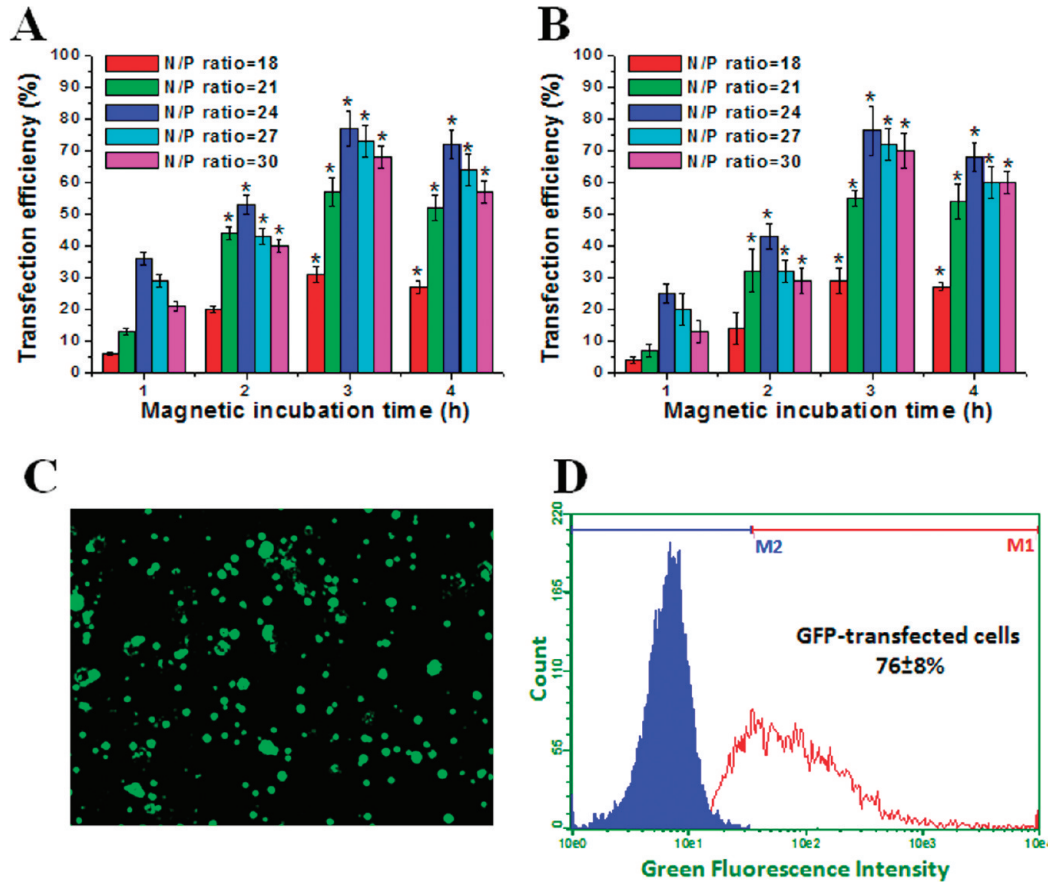

Figure 6. GFP plasmid delivery by PEI-coated SPMNs in 3D cell cultures: (A) transfection efficiency at magnetic incubation time and various N/P ratios determined by fluorescence microscopy; (B) transfection efficiency at magnetic incubation time and various N/P ratios determined by flow cytometric analysis; (C) fluorescent microscopy image of 3D cells transfected by PEI-coated SPMNs/GFP plasmid at N/P ratio of 24 for 3 h; magnification, 100×; (D) flow cytometric analysis of 3D cells transfected by PEI-coated SPMNs/GFP plasmid at N/P ratio of 24 for 3 h. Error bars represent the standard deviation of triplicate biological measurements. The asterisks (*) denote a statistical significance at $P < 0.005$ relative to transfection efficiency at the corresponding N/P ratio at 1 h.

previously transfected by GFP using PEI-coated SPMNs. The complexes were again driven by the external magnetic field for 1, 2, 3, or 4 h. After 24 h incubation at 37 °C, the gene silencing efficiency was evaluated by fluorescence microscopy and flow cytometric analysis. As shown in Figure 8A,B, these transfection complexes showed excellent silencing efficiency for the GFP gene and led to a significant reduction in the population of GFP-expressing cells, with a maximum silencing efficiency (82 ± 4% by fluorescence microscopy image analysis (Figure 8A,C); 80 ± 7% by flow cytometric analysis (Figure 8B,D)) at an N/P ratio of 27 and at 3 h exposure to external magnetic field. Western blotting analysis confirmed the significantly reduced GFP expression after GFP silencing (Figure 8E). This result clearly demonstrates that PEI-coated SPMNs have the potential to be used as an shRNA-plasmid delivery carrier to achieve gene silencing in 3D cell cultures. Similar results were obtained with 3D cultures of other cell types such as CHO K1 cell and HEK 293 cell (Supporting Information, Figure S3), showing the general applicability of the SPMNs for nucleic acid delivery to a variety of cultured mammalian cells. Gene silencing with RNAi has been applied in drug discovery to find and demonstrate gene function and target validation by inhibiting the expression of specific genes, primarily in 2D cell-culture assays. With the development of PEI-

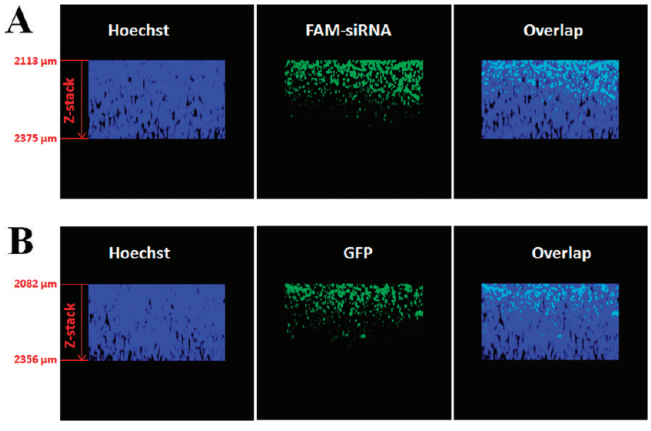

Figure 7. *Z*-stack images of 3D cell cultures transfected by PEI-coated SPMNs/FAM-siRNA or GFP plasmid complexes: (A) 3D cell cultures transfected by PEI-coated SPMNs/FAM-siRNA at N/P ratio of 33 for 3 h; (B) 3D cell cultures transfected by PEI-coated SPMNs/GFP plasmid at N/P ratio of 24 for 3 h. Left hand scale: distance from top of the culture.

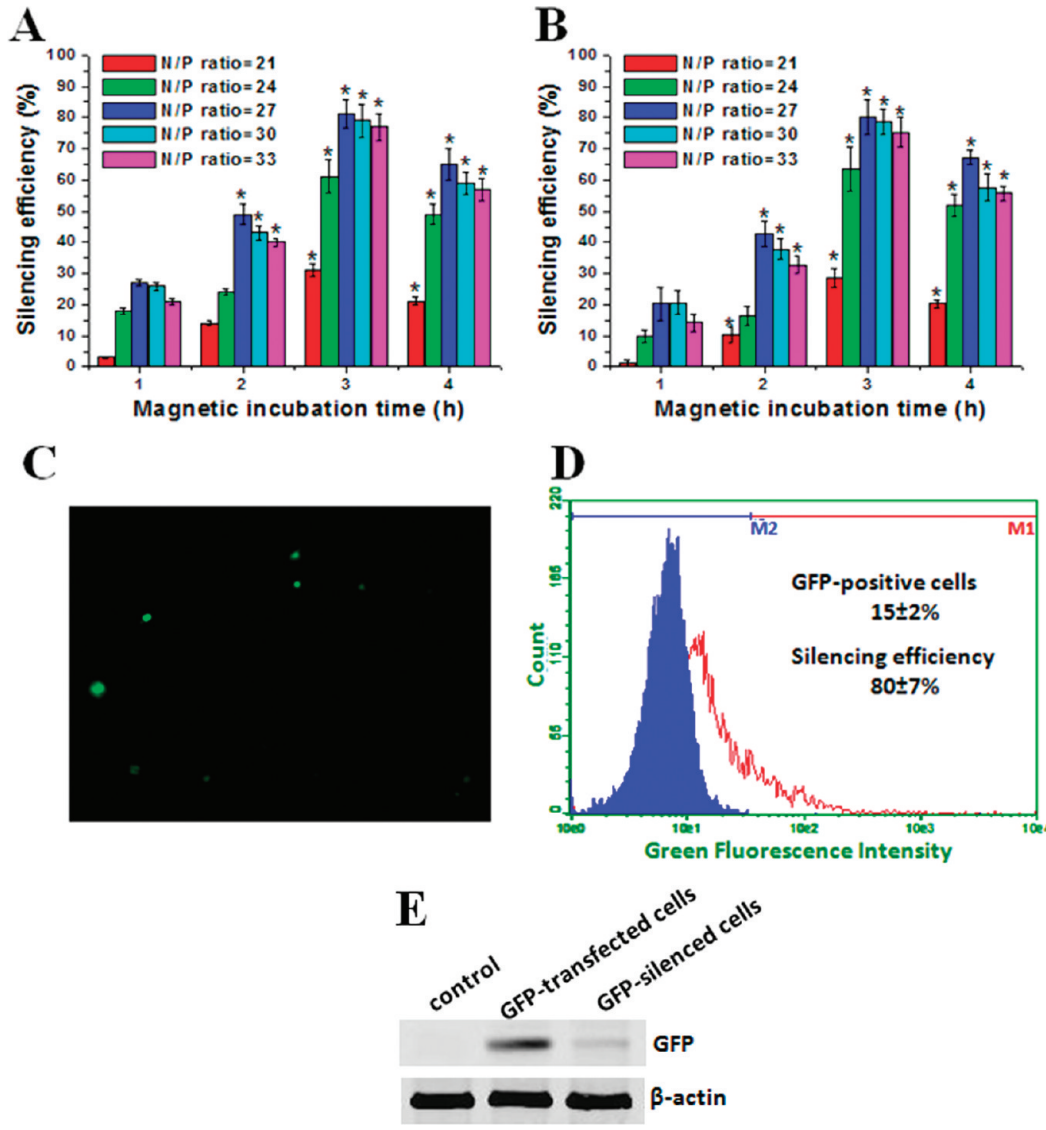

Figure 8. GFP silencing by PEI-coated SPMNs/GFP shRNA in GFP-transfected 3D cell cultures: (A) silencing efficiency at varying magnetic incubation times and N/P ratios determined by fluorescence microscopy; (B) silencing efficiency at varying magnetic incubation times and N/P ratios determined by flow cytometric analysis; (C) fluorescent microscope image of the silenced 3D cell cultures treated by PEI-coated SPMNs/GFP shRNA at N/P ratio of 27 for 3 h; magnification, 100×; (D) flow cytometric analysis of the silenced 3D cell cultures treated by PEI-coated SPMNs/GFP shRNA at N/P ratio of 27 for 3 h; (E) western blotting analysis of GFP protein level in 3D cultures; left lane, control; center lane, GFP-transfected culture (treated by PEI-coated SPMNs/GFP plasmid complexes at N/P ratio of 24 for 3 h); right lane, GFP-silenced culture (treated by PEI-coated SPMNs/GFP shRNA at N/P ratio of 27 for 3 h). Error bars represent the standard deviation of triplicate biological measurements. The asterisks (*) denote a statistical significance at $P < 0.005$ relative to transfection efficiency at the corresponding N/P ratio at 1 h.

coated SPMNs carriers, it is now possible to apply RNAi screening in 3D cellular assays.

Application of Toxic shRNAs with PEI-Coated SPMNs. RNAi therapeutics are a potential new class of pharmaceutical drugs. Some RNAi molecules have shown significant cell toxicities by specifically silencing critical target genes. To demonstrate the ability of our PEI-coated SPMNs to transfect RNAi molecules with significant physiological effects, four known toxic shRNAs, psma 1 shRNA-1, psma 1 shRNA-2, kif 11 shRNA and plk 1 shRNA, were transfected into 2D and 3D cultures of NIH 3T3 cells, and their toxicity was verified by live/dead staining. Plasmids containing these four shRNAs were formed into transfection complexes with PEI-coated SPMNs. On the basis of previous plasmid delivery results, the N/P ratio was fixed at 27 and the external magnetic field was applied for 3 h. After a 24-h incubation, the RNAi toxicities were evaluated using calcein AM and ethidium homodimer-1 staining (Live/Dead Viability/Cytotoxicity Assay Kit), in which live cells exhibit a green fluorescent signal and dead cells a red fluorescent signal. Both calcein AM and ethidium homodimer-1 are low molecular-weight compounds that can easily diffuse into the collagen gel. Live and dead fractions were calculated based on fluorescence microscopy image analysis as described in Materials and Methods. The 2D cell-culture toxicity assay indicated that all four PEI-coated SPMNs/RNAi complexes

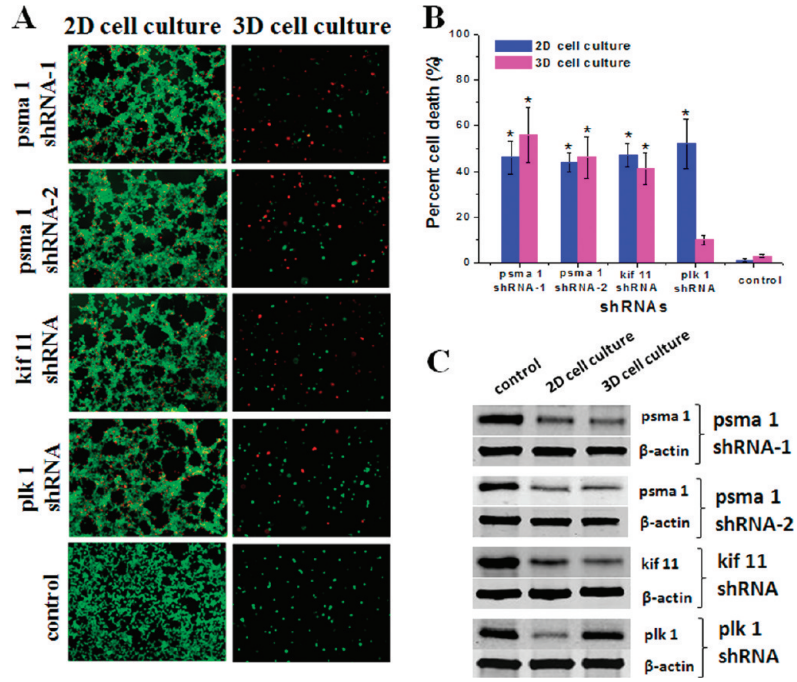

Figure 9. 2D and 3D cellular toxicity assay of toxic shRNA plasmids delivered by PEI-coated SPMNs. 2D and 3D cell cultures were treated with four known toxic shRNA plasmids (psma 1 shRNA-1, psma 1 shRNA-2, kif 11 shRNA and plk 1 shRNA) complexed with PEI-coated SPMNs at an N/P ratio of 27 with 3 h magnetic incubation: (A) fluorescent microscopy images of 2D (left panels) and 3D (right panels) cell cultures; magnification, 100×; (B) percentage of dead cells in 2D and 3D cell culture. Viability was determined by live/dead staining with live cells exhibiting green fluorescence and dead cells red fluorescence. As a control, PEI-coated SPMNs alone were used to treat 2D and 3D cell cultures; (C) Western blotting analysis of psma 1, kif 11 and plk 1 proteins in 2D and 3D cell cultures. Error bars represent the standard deviation of triplicate biological measurements. The asterisks (∗) denote a statistical significance at $P < 0.005$ when compared with control.

killed 44−52% of the cells in 2D culture (46% for psma 1 shRNA-1, 44% for psma 1shRNA-2, 47% for kif 11 shRNA, and 52% for plk 1 shRNA) (Figure 9A, left panels; Figure 9B, blue column), but PEI-coated SPMNs alone caused less than 1% cell death (Figure 9A, bottom left panel; Figure 9B), indicating low toxicity. The 3D cellular toxicity assay indicated that three of the PEI-coated SPMNs/RNAi complexes caused cell death in 41−51% of the cells (51% for psma 1 shRNA-1, 46% for psma 1shRNA-2, and 41% for kif 11 shRNA) while PEI-coated SPMNs alone less caused than 3% cell death (Figure 9A, right panels; Figure 9B, pink column), in agreement with the results of the 2D cellular toxicity assay. Additionally, plk 1 shRNA delivered by PEI-coated SPMNs caused about 10% cell death in the 3D cellular assay, somewhat lower than in the 2D cellular assay. This difference in toxicity may be attributed to differences in cell-culture conditions leading to different physiological responses to silencing of this gene or to a different level of silencing. The gene silencing in 2D and 3D cell cultures was further confirmed by Western blotting analysis which showed reduced protein expression for each of the respective genes (Figure 9C). This preliminary RNAi toxicity assay clearly demonstrates that PEI-coated SPMNs can be used as carriers for screening RNAi molecules in 3D cellular assays, which would greatly broaden the application field of 3D cellular assays beyond small organic molecules to include siRNA molecules and shRNA plasmids.

CONCLUSIONS

PEI-coated SPMNs can stably bind siRNA and plasmid DNA, and efficiently deliver them through a collagen gel matrix allowing them to enter cells in 3D-culture environments. We have successfully applied PEI-coated SPMNs to transfect transgenes into cells grown in a collagen matrix and to modulate the expression of these transgenes with interfering RNA. We have further demonstrated our ability to modulate intrinsic cell physiology by transfecting toxic shRNA molecules into cells grown in a 3D-culture environment. This development provides new opportunities for RNAi screening for therapeutic applications or pathway analysis in 3D cell-culture assays.

MATERIALS AND METHODS

Reagents. Branched polyethylenimine (PEI, 25 kDa) was purchased from Polysciences (Warrington, PA). Iron oxide superparamagnetic nanoparticles (30 nm) coated with oleic acid were purchased from Ocean Nanotech (Springdale, AR). A NdFeB Magnetic plate (1.2 T) was purchased from OZ Biosciences (Parc Scientifique Luminy, France). Carboxyfluorescein (FAM)-labeled siRNA (FAM-siRNA) was purchased from Ambion (Austin, TX). Green fluorescent protein (GFP) and GFP shRNA plasmids were generous gifts from Professor Douglas Conklin (SUNY Albany) and Professor David Schaefer (UC Berkeley), respectively. psma 1 shRNA-1, psma 1 shRNA-2, plk 1 shRNA and kif 11 shRNA indi-

vidual clones were purchased from OpenBiosystems (Huntsville, AL). All plasmids were purified using a Qiagen Plasmid Maxi Kit (Valencia, CA) as per the manufacturer's instructions. Molecular Probes LIVE/DEAD Viability/Cytotoxicity Kit (catalog no. L3224) based on calcein AM and ethidium homodimer-1 staining was purchased from Invitrogen. All other chemical reagents were purchased from Sigma-Aldrich (St. Louis, MO) unless otherwise indicated. Reagent grade water used in all experimental procedure was obtained from a Milli-Q water purification system (Millipore, Bedford MA).

Cell Culture. NIH 3T3 cells (generously provided by Professor George Plopper at RPI) and HEK 293 (ATCC, Manassas, VA) were cultured in Dulbecco's modified Eagle's medium (DMEM) (Hyclone, Logan, UT) supplemented with fetal bovine serum (10%), penicillin (100 U/mL), streptomycin (100 mg/mL), and glutamine (2 mM) (all from Hyclone, Logan, UT) at 37 °C, 5% CO_2. Cells were grown routinely in T-75 tissue culture flasks and passaged by trypsinization. CHO-K1 cells (ATCC, Manassas, VA) were cultured in DMEM/F12 medium (Hyclone, Logan, UT) supplemented with fetal bovine serum (10%), penicillin (100 U/mL), streptomycin (100 mg/mL), and glutamine (2 mM). Cells were grown routinely in T-75 tissue culture flasks and passaged by trypsinization

Preparation of 3D cell cultures. A cell-suspension solution (6×10^5 cells/mL) in ice-cold collagen was prepared by completely mixing 250 μL/well (24-well plate (BD Biosciences, San Jose, CA), surface area, 2 cm^2) of a cell suspension consisting of 9×10^5 cells/mL in DMEM complete medium with 125 μL/well of a type I rat-tail collagen solution (3.9 mg/mL from BD Biosciences). The resulting cell-suspension solution was transferred into a 24-well tissue culture plate. The plate was incubated in a 5% CO_2 incubator at 37 °C for 30 min. After gelation, 400 μL/well of DMEM complete medium was added to the top of the collagen gel, followed by 24 h incubation in the incubator.

Evaluation of Commercial Transfection Reagents. Commercially available transfection reagents (Table 1) were used to form transfection complexes with FAM-siRNA (0.96 μg) or GFP plasmid (1 μg), respectively, according to the respective manufacturer's instructions. The resulting transfection complex was added into one well of a 24-well plate that had previously been plated with a 3D cell culture, as described above. For PolyMag complexes, a NdFeB magnet was placed on the bottom of the 24-well plate in an incubator for 1, 2, 3, or 4 h continuous incubation. Fluorescence images of 3D cell cultures were visualized with a Nikon ECLIPSE TE2000-S fluorescence microscope (Nikon, Melville, NY) and captured with a SPOT-RT digital camera (Diagnostic Instruments, Sterling Heights, MI). The images of 3D cell cultures incubated with transfection reagent/FAM-siRNA complexes were acquired after 4 h incubation and those incubated with transfection reagent/GFP plasmid complexes were acquired after 24 h.

Preparation of PEI-Coated Iron Oxide Superparamagnetic Nanoparticles (PEI-Coated SPMNs). Iron oxide SPMNs coated with PEI were prepared based on a direct ligand-exchange reaction.[22] Branched PEI (25 kDa) with abundant primary and secondary amine groups was used as the multivalent ligand. PEI-coated SPMNs were synthesized at varying reaction ratios (PEI(w)/SPMNs(w) = 2:1, 5:1, and 10:1). Briefly, 10 mL of a solution of iron oxide SPMNs coated with oleic acid (0.1 mg/mL) in anhydrous chloroform was added dropwise to 10 mL of a 0.2 mg/mL (ratio = 2:1) or 0.5 mg/mL (ratio = 5:1) or 1.0 mg/mL (ratio = 10:1) solution of PEI in anhydrous chloroform under an argon atmosphere. The resulting mixture was gently refluxed for 2 h and stirred at room temperature for 24 h under argon. The volume was reduced to 5 mL by evaporation under argon flow, and 15 mL of hexane was added to this solution. The precipitate was collected by filtration, washed with diethyl ether, dried under vacuum, and then dissolved in water. Free unbound PEI polymers were removed by dialysis (MW cutoff = 50 kDa) against deionized water. The dialysis solution was lyophilized and the iron content was determined using an inductively coupled plasma optical emission spectrometer (Varian 700-ES, Palo Alto, CA) and the nitrogen content was determined by elemental analysis (Perkin-Elmer 2400, Norwalk, CT). The transmission electron microscopy (TEM) images of PEI-coated SPMNs were obtained on a Philips CM 120 electron microscope operated at 120 keV. The hydrodynamic particle sizes and zeta potentials of the PEI-coated SPMNs were determined in 5% glucose aqueous solution by dynamic lighting scattering (DLS) using a Dynapro Titan (Wyatt technology, Santa Barbara, CA) and Zetasizer Nano Z (Malvern Instruments, Herrenberg, Germany), respectively.

Preparation of Magnetic PEI-Coated SPMN/Nucleic Acid Complexes. Magnetic PEI-coated SPMNs/nucleic acid complexes were formed at various N/P (nitrogen in PEI-coated SPMN/phosphorus in DNA or RNA) ratios by mixing various volumes of the aqueous solution of PEI-coated SPMNs (3.1 mg/mL, formed at a reaction ratio of 2:1 PEI:SPMN) with 1 μL plasmid solution (1 μg/μL) or 12 μL FAM-labeled siRNA (0.08 μg/μL) in 400 μL transfection buffer (10 mM HEPES, pH 7.4, 50 mM NaCl, 5% glucose). The resulting solutions were gently pipetted up and down five times and incubated for 20 min at room temperature. The hydrodynamic particle sizes and zeta potentials of the transfection complexes were determined as described for the SPMNs above.

Gel Electrophoresis Retardation Assay. The ability of the complexes to retard DNA migration was measured by agarose electrophoresis in a horizontal gel electrophoresis system (Biorad). The magnetic PEI-coated SPMN/siRNA or PEI-coated SPMN/GFP plasmid transfection complexes formed at various N/P ratios were loaded onto a 3% agarose gel for the siRNA assay or a 0.9% agarose gel for the GFP assay. The loading amount in each lane was 0.5 μg of nucleic acid for siRNA or 1 μg of nucleic acid for GFP plasmid. Gel electrophoresis was carried out at room temperature in 1× TAE buffer at 5.3 V/cm for 60 min. The RNA or DNA bands were visualized by UV illumination of ethidium−bromide-stained gels and captured using a ChemiImager 4400 Gel imaging system (Alpha Innotech, San Leandro, CA).

Delivery of FAM-siRNA, GFP Plasmid and GFP shRNA Plasmid into 3D Cell Cultures. The medium on the top of the collagen gel was replaced with 400 μL/well of a solution of PEI-coated SPMNs complexed with FAM-siRNA or GFP plasmid (described above) and a NdFeB magnet was placed on the bottom of the 24-well plate in incubator for 1, 2, 3, or 4 h continuous incubation. Fluorescence images of 3D cell cultures were visualized with a Nikon ECLIPSE TE2000-S fluorescence microscope (Nikon, Melville, NY) and captured with a SPOT-RT digital camera (Diagnostic Instruments, Sterling Heights, MI). For FAM-siRNA delivery; fluorescence images were acquired as soon as the magnet was removed. For GFP plasmid delivery, fluorescence images were acquired after an additional 24-h incubation with fresh DMEM complete medium without the external magnetic field. The GFP-transfected 3D cell cultures were further silenced after 24 h by subsequently applying 400 μL of a solution of PEI-coated SPMN/GFP shRNA plasmid complexes as described above. The green fluorescence intensity was quantified from the microscopic images with Photoshop (Adobe System, San Jose, CA) using the histogram function.[24] Transfection efficiency was evaluated using $[(F_{Sam} - F_{Min}) \times T\%]/(F_T - F_{Min})$, where F_{Sam} is the green fluorescence intensity of the sample cells gel; F_T is the green fluorescence intensity of a population of cells with known transfection efficiency (T%) (based on fluorescence-activated cell sorting) that were subsequently placed into a collagen gel; F_{Min} is the green fluorescence intensity of untransfected cells. Silencing efficiency was evaluated by $[(F_H - F_{Min}) - (F_{Sam} - F_{Min})] \times 100\%/(F_H - F_{Min})$, where F_{Sam} is the green fluorescence intensity of the sample cells gel; F_H is the green fluorescence intensity of cells in the gel at the highest transfection efficiency; F_{Min} is the green fluorescence intensity of untransfected cells.

Flow Cytometry Analysis. The collagen gel for each 3D cell culture in 24-well plate was degraded to release the individual cells by incubating with 400 μL of DMEM medium containing 50 U/mL of collagenase I (Worthington Biochemical Corporation, Lakewood, NJ) and 5 mM of $CaCl_2$, followed by 1 h incubation at 37 °C. The cells were harvested by centrifugation at 1000 rpm for 15 min, washed twice with 500 μL of PBS, and resuspended in 500 μL of PBS. The resulting cell suspensions were analyzed by flow cytometry on a Guava Easycyte Mini System (Guava Technologies, CA); 5000 events were analyzed for fluorescence signals. The transfection efficiency was calculated as the percentage of the fluorescence-emitting cells in the total number of cells. Transfection efficiency (T) was evaluated by the percentage of green fluorescence labeled cells in total cells. Silencing ef-

ficiency was determined by $[(T_{Bef} - T_{Aft}) \times 100\%]/T_{Bef}$, where T_{Bef} is the transfection efficiency before knockdown; T_{Aft} is the transfection efficiency after knockdown.

Z-Stack Confocal Image Analysis. A 200 μL portion of a 3D cell culture (prepared as described above) was transferred into one chamber (surface area: 0.8 cm^2/well) of a Lab-Tek eight-chambered coverglass (Fisher Scientific, Pittsburgh, PA), followed by 3 h of magnetic transfection using 160 μL of transfection complexes as described above (samples transfected with GFP plasmids were then incubated for an additional 24 h before imaging). The transfected 3D culture was washed twice with 200 μL of PBS, and cell nuclei were stained with 200 μL of 1 μM of Hoechst 33342 in PBS for 30 min. The staining solution was discarded and the gel surface was washed twice by 200 μL of PBS solution. Z-stack of 3D cultures were acquired using Leica confocal multiphoton-FLIM microscope (Leica Laser Technik GmbH, Heidelberg, Germany) with a long-distance water-immersion objective (20×) through a section thickness of 2.53 μm.

Delivery and Cytotoxicity Assay of Toxic shRNA Molecules. The medium on the top of the collagen gel was replaced with 400 μL of a solution of PEI-coated SPMNs complexed with psma 1 shRNA-1, psma 1 shRNA-2, plk 1 shRNA, or kif 11 shRNA plasmids. As a control, 400 μL of transfection buffer containing PEI-coated SPMNs was added to the top of collagen gel. A NdFeB magnet was placed on the bottom of the 24-well plate in the incubator for 1, 2, 3, or 4 h of continuous incubation. After an additional 24-h incubation with fresh DMEM complete medium without the external magnetic field, the medium was removed and 5 μL of calcein AM (4 mM) and 10 μL of ethidium homodimer (2 mM) were mixed in 2 mL of phosphate buffered saline (PBS); 400 μL of this mixture was added to the top of the collagen gel, and 3D cell cultures were stained for 30 min at room temperature. The live cells (green fluorescence) and dead cells (red fluorescence) were detected by fluorescence microscopy. For comparison, a 2D cellular assay was also performed. In this assay, 2.4×10^5 cells were seeded in each well of a 24-well plate and incubated for 24 h in incubator at 37 °C, 5% CO_2. The medium was removed and 400 μL of a solution of PEI-coated SPMNs complexed with toxic shRNA plasmids or PEI-coated SPMNs was added to the top of the cell monolayer, after which the external field was applied for 15 min followed by 4 h of incubation. The transfection complexes were replaced with 400 μL of fresh DMEM complete medium, and the cultures were incubated for 24 h. The medium was subsequently removed; 400 μL of the calcein/ethidium homodimer/PBS solution described above was added to the surface of 2D cell cultures, and the cells were stained for 30 min at room temperature. The live cells (green fluorescence) and dead cells (red fluorescence) were detected by fluorescence microscopy. The toxicities of the RNAi molecules were evaluated by the percentage of dead cells. The red fluorescence intensity is linearly proportional to the total number of dead cells and was quantified from the microscopic images with Photoshop using the histogram function.[24] Dead cells % $= [(F_{Sam} - F_{Min})/(F_{Max} - F_{Min})] \times 100\%$, where F_{Sam} is the red fluorescence intensity of the sample cells, F_{Max} is the red fluorescence intensity of 100% dead cells (after treatment with 70% methanol for 1 h), and F_{Min} is the red fluorescence intensity of untreated fully viable cells.

Western Blot Analysis. The collagen was degraded to release the transfected cells from the 3D cell culture as described above. The cells were harvested by centrifugation at 1000 rpm for 15 min, washed twice with 500 μL of PBS, and lysed with ice-cold RIPA buffer (50 mM Tris-HCl, pH 7.5, 150 mM NaCl, 1% Nonidet P-40, 0.5% sodium deoxycholate, 0.1% sodium dodecyl sulfate) containing 1 mM phenylmethyl sulfonyl fluoride. The lysate was incubated on ice for 20 min, followed by sonication for 5 s, and further incubated for another 20 min on ice. The lysate was then centrifuged at 10000 rpm in a microcentrifuge tube for 10 min, and the protein concentration in the supernatant was determined using the Bio-Rad DC protein assay kit (Bio-Rad, Hercules,CA). Equal amounts of protein (50 μg) were separated on 10% sodium dodecyl sulfate−polyacrylamide gels and transferred onto nitrocellulose membrane. The membrane was blocked with 5% nonfat dry milk in TBS/T (Tris buffered saline containing 0.1% v/v Tween-20) buffer for 1 h at room temperature, and then probed with the following primary antibodies in TBS/T buffer containing 2% nonfat dry milk for 1 h at room temperature. Mouse anti-kif11 monoclonal antibody (1:1000) and mouse anti-plk1 monoclonal antibody (1:1000) were purchased from Biolegend (San Diego, CA). Rabbit anti-psma1 polyclonal antibody (1:500), mouse anti-GFP monoclonal antibody (1:200), and mouse anti-β-actin monoclonal antibody (1:1000) were purchased from Santa Cruz Biotechnology (Santa Cruz, CA). After being washed twice at 10-min intervals with TBS/T solution, the membrane was incubated with goat antirabbit or goat anti-mouse horseradish peroxidase-conjugated secondary antibody (1:1000) (Santa Cruz, CA) in TBS/T buffer containing 2% of nonfat dry milk for 1 h at room temperature. After washing twice at 10-min intervals with TBS/T buffer, the immunoreactivity of protein on the membrane was visualized by chemoluminescence using an enhanced Immun-Star HRP chemoluminescence kit (Bio-Rad, Hercules,CA).

Statistical Analysis. All data were expressed as mean ± SD. All values were obtained from at least three independent experiments. Statistical significance was evaluated using two-tailed heteroscedastic Student's *t*-tests according to the TTEST function in Microsoft Excel. The difference between groups was considered statistically significant when the *P*-value was less than 0.05.

Acknowledgment. This work was supported by a grant from the National Science Foundation to Solidus Biosciences, Inc. (IIP-0740592). The authors would like to thank Drs. Joel Morgan, Fuming Zhang, Duan Shen, Xi Li, and Yongquan Qu for assistance with experimental procedures.

Supporting Information Available: A table containing sizes and zeta potentials of PEI coated-SPMNs complexed with siRNA and GFP plasmid DNA, images of time-dependent transfection at differential depths obtained by confocal microscopy, and fluorescence micrographs of GFP plasmid transfection and GFP silencing in additional cell lines. This material is available free of charge *via* the Internet at http://pubs.acs.org.

REFERENCES AND NOTES

1. Burbaum, J.; Tobal, G. M. Proteomics in Drug Discovery. *Curr. Opin. Chem. Biol.* **2002**, *6*, 427–433.
2. Kramer, R.; Cohen, D. Functional Genomics to New Drug Targets. *Nat. Rev. Drug. Discovery* **2004**, *3*, 965–972.
3. Onyango, P. The Role of Emerging Genomics and Proteomics Technologies in Cancer Drug Target Discovery. *Curr. Cancer Drug Targets* **2004**, *4*, 111–124.
4. Gupta, P.; Lee, K. H. Genomics and Proteomics in Process Development: Opportunities and Challenges. *Trends Biotechnol.* **2007**, *25*, 324–330.
5. Dobson, C. M. Chemical Space and Biology. *Nature* **2004**, *432*, 824–826.
6. Service, R. F. Surviving the Blockbuster Syndrome. *Science* **2004**, *303*, 1796–1799.
7. Billingsley, M. L. Druggable Targets and Targeted Drugs: Enhancing the Development of New Therapeutics. *Pharmacology* **2008**, *82*, 239–244.
8. Lindsay, M. A. Target Discovery. *Nat. Rev. Drug Discovery* **2003**, *2*, 831–838.
9. Knowles, J.; Gromo, G. A Guide to Drug Discovery: Target Selection in Drug Discovery. *Nat. Rev. Drug Discovery* **2003**, *2*, 63–69.
10. Abbott, A. Biology's New Dimension. *Nature* **2003**, *424*, 870–872.
11. Cheng, K.; Lai, Y.; Kisaalita, W. S. Three-Dimensional Polymer Scaffolds for High Throughput Cell-Based Assay Systems. *Biomaterials* **2008**, *29*, 2802–2812.
12. Sivaraman, A.; Leach, J.; Townsend, S.; Iida, T.; Hogan, B.; Stolz, D.; Fry, R.; Samson, L.; Tannenbaum, S.; Griffith, L. A Microscale *in Vitro* Physiological Model of the Liver: Predictive Screens for Drug Metabolism and Enzyme Induction. *Curr. Drug Metab.* **2005**, *6*, 569–591.
13. Yamada, K. M.; Clark, K. Cell Biology: Survival in Three Dimensions. *Nature* **2004**, *419*, 790–791.

14. Ostrovidov, S.; Jiang, J.; Sakai, Y.; Fujii, T. Membrane-Based PDMS Microbioreactor for Perfused 3D Primary Rat Hepatocyte Cultures. *Biomed. Microdevices* **2004**, *6*, 279–287.
15. Pampaloni, F.; Reynaud, E.; Stelzer, E. The Third Dimension Bridges the Gap between Cell Culture and Live Tissue. *Nat. Rev. Mol. Cell Biol.* **2007**, *8*, 839–845.
16. Lee, M. Y.; Kumar, R. A.; Sukumaran, S. M.; Hogg, M. G.; Clark, D. S.; Dordick, J. S. Three-Dimensional Cellular Microarray for High-throughput Toxicology Assays. *Proc. Natl. Acad. Sci. U.S.A.* **2008**, *105*, 59–63.
17. Bumcrot, D.; Manoharan, M.; Koteliansky, V.; Sah, D. W. Y. RNAi Therapeutics: A Potential New Class of Pharmaceutical Drugs. *Nat. Chem. Biol.* **2006**, *2*, 711–719.
18. Leung, R. K. M.; Whittaker, P. A. RNAi Interference: From Gene Silencing to Gene-Specific Therapeutics. *Pharmacol. Ther.* **2005**, *107*, 222–239.
19. Kumar, R.; Conklin, D. S.; Mittal, V. High-Throughput Selection of Effective RNAi Probes for Gene Silencing. *Genome Res.* **2003**, *13*, 2333–2340.
20. Silva, J. M.; Mizuno, H.; Brady, A.; Lucita, R.; Hannon, G. J. RNA Interference Microarrays: High-Throughput Loss-of-Function Genetics in Mammalian Cells. *Proc. Natl. Acad. Sci. U.S.A.* **2004**, *101*, 6548–6552.
21. Wheeler, D. B.; Bailey, S. N.; Guertin, D. A.; Carpenter, A. E.; Higgins, C. O.; Sabatini, D. M. RNAi Living-Cell Microarrays for Loss-of-Function Screens in Drosophila Melanogaster Cells. *Nat. Methods* **2004**, *1*, 127–132.
22. Duan, H.; Kuang, M.; Wang, X.; Wang, Y. A.; Mao, H.; Nie, S. Reexamining the Effects of Particle Size and Surface Chemistry on the Magnetic Properties of Iron Oxide Nanocrystals: New Insights into Spin Disorder and Proton Relaxivity. *J. Phys. Chem. C* **2008**, *112*, 8127–8131.
23. Boussif, O.; Lezoualc'h, F.; Zanta, M. A.; Mergny, M. D.; Scherman, D.; Demeneix, B.; Behr, J. P. A Versatile Vector for Gene and Oligonucleotide Transfer into Cells in Culture and *in Vivo*: Polyethylenimine. *Proc. Natl. Acad. Sci. U.S.A.* **1995**, *92*, 7297–7301.
24. Lee, M. Y.; Park, C. B.; Dordick, J. S.; Clark, D. S. Metabolizing Enzyme Toxicology Assay Chip (MetaChip) for High-Throughput Microscale Toxicity Analyses. *Proc. Natl. Acad. Sci. U.S.A.* **2005**, *102*, 983–987.